International Forum on Aeroelasticity and Structural Dynamics
IFASD 2024
17-21 June 2024, The Hague, The Netherlands

AERODYNAMIC ANALYSIS OF AIRCRAFT WINGS USING A COUPLED PM-BL APPROACH

Lipeng Zhu [1], Changchuan Xie [1,2], Yang Meng [1]

[1] Beihang University, China

[2] Hangzhou International Innovation Institute, Beihang University, China

Keywords: Panel Method, Unsteady Boundary Layer Method, Viscous Correction

Abstract: The objective of this paper is to develop an aerodynamic model suitable for aeroelastic analysis with low computational cost and sufficient fidelity. The physics-based reduce order model is based on the unsteady inviscid Panel Method (PM), selected for its low computation time. Viscous effects are modeled with two-dimensional unsteady high-fidelity boundary layer calculations at various sections along the span and incorporated as an effective shape boundary condition correction inside the PM. The viscous sectional data are calculated with two-dimensional differential boundary layer equations to allow viscous effects to be included for a more accurate maximum lift coefficient and spanload evaluations. These viscous corrections are coupled through a modified displacement thickness distribution coupling method for 2D boundary layer sectional data.

1 INTRODUCTION

With the improvement of high lift-to-drag ratio, long endurance, and other performance index requirements, and the increasing use of lightweight composite materials in aircraft, there has been rapid development in recent years of high aspect ratio wing layout aircraft. This development is particularly evident in high-altitude and long endurance unmanned aerial vehicles (UAVs) and large-scale transport aircraft. However, this advancement also brings about more complex aeroelastic problems and challenges. Flexible aircraft with high aspect ratio often experience significant structural deformation under aerodynamic load, and the geometric nonlinear aeroelastic effect is pronounced. Traditional aeroelastic analysis methods based on linear small deformation assumptions are no longer sufficient to provide accurate calculation results or accurately depict real physical scenarios. Therefore, the development of aeroelasticity research methods considering geometric nonlinear effects for large flexible aircraft has become a crucial research direction in aircraft design.

One of the key aspects in the geometrically nonlinear aeroelastic problem is aerodynamic modeling. In this scenario, the large deformation of the structure results in an increase in the local angle of attack, leading to a significant rise in the influence of viscous effects. As a consequence, the accuracy of the traditional potential flow theory analysis becomes insufficient to meet the required standards. Incorporating the high-precision CFD analysis method not only leads to a significant increase in calculation time but also escalates the complexity of integrating the aerodynamic

equation with the structural dynamics equation. The boundary layer approach not only significantly simplifies the Navier-Stokes equations, but also allows for representing viscous effects as a source distribution, consistent with the singularity element form of potential flow theory.Therefore, the viscous correction of potential flow theory can be achieved with minimal computational effort, making it highly suitable for aerodynamic modeling and analysis of geometrically nonlinear aeroelastic problems.

The fidelity of the method has been validated against solutions obtained from a 3D RANS flow solver on a high aspect ratio wing. The results demonstrate a remarkable level of accuracy in the coupled PM-BL approach when compared to 3D RANS solutions, with computation times in the order of minutes on a standard desktop computer. These findings underscore the precision and efficiency of the coupled PM-BL method in aerodynamic simulations.

2 TWO-DIMENSIONAL BOUNDARY-LAYER METHODS

The concept of eddy-viscosity (ε_m) is utilized in solving the boundary-layer equations for turbulent flow,

$$-\rho\overline{u'v'} = \rho\varepsilon_m \frac{\partial u}{\partial y} \tag{1}$$

in this way, the solution procedure for the momentum equation and continuity equation, Eq. (2),

$$\begin{gathered} \frac{\partial u}{\partial x} + \frac{\partial v}{\partial y} = 0 \\ \frac{\partial u}{\partial t} + u\frac{\partial u}{\partial x} + v\frac{\partial u}{\partial y} = \frac{\partial u_e}{\partial t} + u_e\frac{\partial u_e}{\partial x} + \nu\frac{\partial}{\partial y}\left(b\frac{\partial u}{\partial y}\right) \end{gathered} \tag{2}$$

is the same for both laminar and turbulent flows, utilizing an algebraic eddy-viscosity formulation, where $b = 1 + \varepsilon_m^+, \varepsilon_m^+ = \dfrac{\varepsilon_m}{\nu}$.

The eddy viscosity variables are effectively represented using the Cebeci-Smith (CS) algebraic formulation[1]. This model conceives the turbulent boundary layer as a composite structure comprising inner and outer regions, each defined by a unique expression.

In the inner region, the eddy-viscosity formula is defined by

$$\left(\varepsilon_m\right)_i = L^2\left|\frac{\partial u}{\partial y}\right|\gamma_{tr}, \quad 0 \le y \le y_c \tag{3}$$

where

$$\begin{gathered} L = \kappa y\left[1 - \exp\left(-y/A\right)\right] \\ A = 26\frac{\nu}{u_\tau}, \quad u_\tau = \left(\frac{\tau}{\rho}\right)_{\max}^{1/2} \end{gathered} \tag{4}$$

In the outer region, the eddy-viscosity formula is defined by

$$\begin{gathered} \left(\varepsilon_m\right)_o = \alpha\left|\int_0^\delta \left(u_e - u\right)dy\right|\gamma_{tr}\gamma \quad y_c \le y \le \delta \\ \alpha = \frac{0.0168}{F^{1.5}} \end{gathered} \tag{5}$$

The parameter *F* is related to the ratio of the product of the turbulence energy by normal stresses to that by shear stress evaluated at the location where the shear stress is maximum.

$$F = 1 - \beta \left(\frac{\partial u / \partial x}{\partial u / \partial y} \right)_{\left(-\rho \overline{u'v'}\right)_{\max}} \tag{6}$$

Here the parameter β is a function of $R_t = \tau_w \Big/ \left(-\rho \overline{u'v'}\right)_{\max}$, which is represented by

$$\beta = \begin{cases} \dfrac{6}{1 + 2R_t \left(2 - R_t\right)} & R_t \le 1.0 \\ \dfrac{1 + R_t}{R_t} & R_t \ge 1.0 \end{cases} \tag{7}$$

For $\tau_w < 0$, R_t is set equal to zero.

The intermittency expression γ is based on Fiedler and Head's correlation and is given by

$$\gamma = \frac{1}{2} \left[1 - erf \frac{\left(y - Y\right)}{\sqrt{2}\sigma} \right] \tag{8}$$

Here *Y* and σ are general intermittency parameters with *Y* denoting the value of *y* where $\gamma = 0.5$ and σ denoting the standard deviation.

The condition used to define y_c in Eqs. (3) and (4) are the continuity of the eddy viscosity, so that ε_m is defined by $\left(\varepsilon_m\right)_i$ from the wall outward (inner region) until its value is equal to that given for the outer region by $\left(\varepsilon_m\right)_o$.

The expression γ_{tr} models the transition region and is given by

$$\gamma_{tr} = 1 - \exp\left(-G\left(x - x_{tr}\right) \int_{x_{tr}}^{x} \frac{dx}{u_e} \right) \tag{9}$$

Here x_{tr} denotes the onset of transition and *G* is defined by

$$G = \frac{3}{C^2} \frac{u_c^3}{\nu^2} R_{x_{tr}}^{-1.34} \tag{10}$$

where *C* is 60 for attached flows and $R_{x_{tr}} = \left(u_e x / \nu\right)_{tr}$ is the transition Reynolds number. In the low Reynolds number range from $R_c = 2 \times 10^5$ to 6×10^5, the parameter *C* is given by

$$C^2 = 213\left(\log R_{x_{tr}} - 4.7323\right) \tag{11}$$

The steady lift coefficient of the NACA0012 airfoil calculated by the boundary-layer method is shown in Fig.1(a), which calculated the working condition is $Re = 3.0 \times 10^6$ and the angle of attack ranges from 0 to 17 degrees. The unsteady analysis results are shown in Fig.1(b), which calculated the working condition is $Re = 3.42 \times 10^5$ and the angle of attack varies with time as $\alpha = 5^\circ + 5^\circ sin0.1t$ .By comparing the analytical results of the panel method, CFD and experiments, it can be seen that the boundary-layer method has the advantages of high fidelity and high computational efficiency.

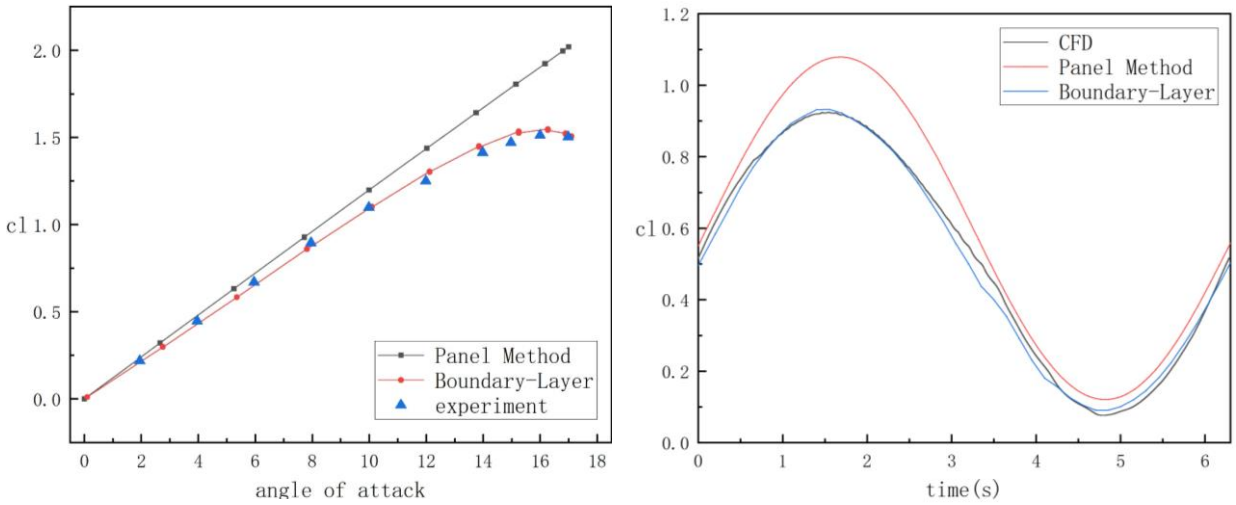

$(a)\, Re = 3.0\times10^{6}$ $(b)\, Re = 3.42\times10^{5}, \alpha = 5^{\circ} + 5^{\circ} sin0.1t$

Figure 1 Analysis results of boundary-layer method

3 THREE-DIMENSIONAL PANEL METHOD AND VISCOSITY CORRECTION

For incompressible irrotational flow, the full velocity potential equation is

$$\frac{\partial^2\Phi}{\partial x^2}+\frac{\partial^2\Phi}{\partial y^2}+\frac{\partial^2\Phi}{\partial z^2}=0 \tag{12}$$

Eqs. (12) is the Laplace equation of the flow, which is satisfied by incompressible potential flows in both steady and unsteady cases. The equation is a linear partial differential equation, and the velocity distribution of the flow field can be solved with specific boundary conditions. In practice, the velocity potential function at any point of the flow field can be written in the following form

$$\Phi(x,y,z)=\frac{1}{4\pi}\int_{S_B+S_W}\mu\boldsymbol{n}\cdot\nabla\frac{1}{r}dS-\frac{1}{4\pi}\int_{S_B}\sigma\left(\frac{1}{r}\right)dS+\Phi_{\infty} \tag{13}$$

As shown in Fig.2, S_{∞}, S_B, S_W are the far field boundary, wall boundary and wake boundary respectively, and $\boldsymbol{n}$ is the normal vector. The panel method is to simulate the flow field characteristics by arranging reasonable basic solutions. The source can be used to model the thickness effect, and the vortex or doublet can be used to model the lift effect. The velocity potential function in the form of Eqs. (13) naturally satisfies Laplace equation (12), and then the strength of each singularity element can be obtained by substituting the boundary conditions and the Kutta conditions, which is the basic idea of the panel method.

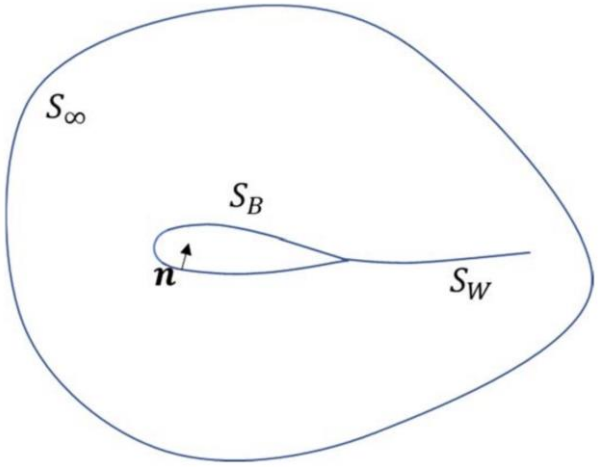

Figure 2 Flow field diagram

The full velocity potential can be divided into disturbance velocity potential and far-field velocity potential.

$$\Phi = \Phi^* + \Phi_\infty \tag{14}$$

First, the boundary condition requires that the wing disturbance at infinity be zero.

$$\lim_{r\to\infty} \nabla\Phi^* = 0 \tag{15}$$

The boundary conditions of the wing wall can be divided into Neumann boundary conditions and Dirichlet boundary conditions, or a mixture of the two combined [2], the Neumann boundary condition requires that the normal velocity at the wall be zero.

$$\nabla\left(\Phi^* + \Phi_\infty\right)\cdot\boldsymbol{n} = 0 \tag{16}$$

The Dirichlet boundary condition requires that the external flow of the closed boundary has no effect on the internal flow, that is, the internal velocity potential remains constant

$$\Phi_{in} = const \tag{17}$$

Different values of this constant can result in different solutions. In more cases, the internal velocity potential is equal to the far-field velocity potential, that is

$$\Phi_{in} = \left(\Phi^* + \Phi_\infty\right)_{in} = \Phi_\infty \tag{18}$$

The Dirichlet boundary condition Eqs. (18) is used in the 3D panel method.

$$\frac{1}{4\pi}\int_{S_B+S_W} \mu\frac{\partial}{\partial n}(\frac{1}{r})dS - \frac{1}{4\pi}\int_{S_B}\sigma\frac{1}{r}dS = 0 \tag{19}$$

Where μ is the doublet strength and σ is the source strength. As shown in Fig.3, the aerodynamic coordinate system is defined: *the x-axis* is along the direction of far flow, the *y-axis* is horizontal to the right, and *the z-axis* is determined by the right-hand rule.

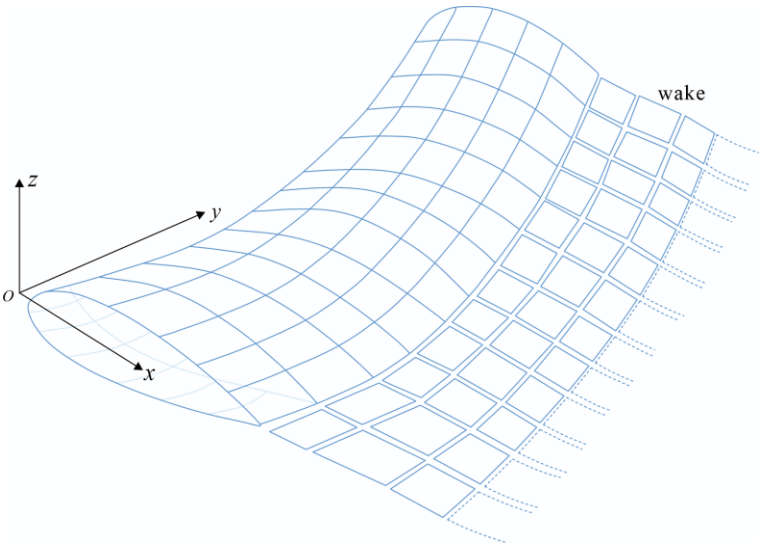

Figure 3 Three-dimensional panel method of mesh division

The upper and lower surfaces of the wing are divided into several quadrilateral grids, each grid of the wing surface is arranged with a continuous distribution of sources and doublets, and only doublets are arranged at the wake mesh. There are N meshes on the wing and $N_w = N_{span} + M_w$ meshes in the wake part. In order to obtain the unique solution of Eqs. (19), the source strength is obtained directly with Neumann boundary conditions:

$$\frac{\partial \Phi}{\partial n} = -\boldsymbol{n} \cdot \boldsymbol{V} \tag{20}$$

According to the characteristics of the source,

$$-\sigma = \frac{\partial \Phi}{\partial n} - \frac{\partial \Phi}{\partial n} = \frac{\partial \Phi^*}{\partial n} - \frac{\partial \Phi_i^*}{\partial n} \tag{21}$$

Since the internal velocity potential is constant, the source strength is

$$\sigma = \boldsymbol{n} \cdot \boldsymbol{V} \tag{22}$$

After the discretization of Eqs. (19), the boundary condition equation at the i th wing grid control point can be obtained:

$$\sum_{k=1}^{N} C_{ik}\mu_k + \sum_{l=1}^{N_w} C_{il}\mu_l + \sum_{k=1}^{N} B_{ik}\sigma_k = 0 \tag{23}$$

where C_{ik}, C_{il} is the influence coefficient of the k-th wing surface doublet mesh and the l-th wake doublet mesh on the i-th wing control point respectively, and B_{ik} is the influence coefficient of the k-th wing surface source mesh on the i-th wing control point, which can be obtained by the following integral equation [2] :

$$\begin{aligned} C_k &= \frac{1}{4\pi} \int \frac{\partial}{\partial n}\left(\frac{1}{r}\right) dS \,|_k \\ B_k &= -\frac{1}{4\pi} \int \left(\frac{1}{r}\right) dS \,|_k \end{aligned} \tag{24}$$

In order to satisfy the Kutta condition, the strength of the latest row of wake doublets generated by the trailing edge at time *t* is the difference of the strength of the upper and lower wing doublets

$$\mu_w^t = \mu_u^t - \mu_l^t \tag{25}$$

In each discrete time step, the wing flies forward at flight speed, and a row of wake meshes emerges from the trailing edge of the wing. Taking the unsteady case of sudden acceleration of the wing from rest as an example, at the 0th time step $t = 0$, there is only one row of wake mesh at the trailing edge of the wing, and the length of the mesh is $0.2 \sim 0.3\boldsymbol{V}\Delta t$. When the first time step $t = \Delta t$, the wing flies a distance of $\boldsymbol{V}\Delta t$ in front, and a doublet element is formed at the trailing edge, and the doublet strength is equal to the trailing doublet strength of the previous time step. In the subsequent time step, the doublet element moves according to the local velocity and maintains the same strength according to Helmholtz's theorem. Considering the Eqs.(25), the boundary condition Eqs.(23) can be rewritten as

$$\sum_{k=1}^{N} A_k \mu_k + \sum_{l=1}^{M_w} C_l \mu_l + \sum_{k=1}^{N} B_k \sigma_k = 0 \tag{26}$$

Where M_w is the number of wake meshes except the newly generated row of trailing wake meshes. For general wing meshes except for trailing edges, $A_k = C_k$; For upper wing trailing edge meshes, $A_k = C_k + C_l$; For lower wing trailing edge meshes, $A_k = C_k - C_l$. Solving the boundary condition Eqs.(26) at each time step yields the fundamental solution strength for all elements.

After the strength of the doublet and the source is obtained, the disturbance velocity of the element surface is also obtained according to the characteristics of this fundamental solution, the tangential velocity is

$$q_l = \frac{\partial \mu}{\partial l}, q_m = \frac{\partial \mu}{\partial m} \tag{27}$$

and normal velocity $q_n = \sigma$ cancel with the normal component of the far flow velocity. Therefore, the actual tangential velocity on the surface of the element is the sum of the tangential component of the far flow velocity and the tangential disturbance velocity:

$$\boldsymbol{Q}_k = [U(t), V(t), W(t)]_k \cdot (l, m, n)_k + \left(q_l, q_m, q_n\right)_k \tag{28}$$

The pressure coefficient of each element is obtained from the unsteady Bernoulli equation:

$$C_{pk} = 1 - \frac{Q_k^2}{Q_\infty^2} - \frac{2}{Q_\infty^2}\frac{\partial \Phi}{\partial t} \tag{29}$$

Where Q_∞ is the magnitude of the velocity of the far flow. The time derivative of the velocity potential is equivalent to the time derivative of the doublet strength:

$$\frac{\partial \Phi}{\partial t} = \frac{\partial \mu}{\partial t} \tag{30}$$

Finally, the aerodynamic force on each element is the product of pressure and area:

$$\boldsymbol{F}_k = -C_{pk}\left(\frac{1}{2}\rho Q_\infty^2\right)\Delta S_k \boldsymbol{n}_k \tag{31}$$

The 3D panel method is limited to the potential flow region and does not account for viscous effects. It results in significant calculation errors when applied to flow fields with prominent boundary layer thicknesses. Consequently, it is unsuitable for such scenarios. The formation of a boundary layer on the surface causes the potential flow outside of it to be displaced into the fluid on a surface located a distance equal to the displacement thickness δ^*. This displacement thickness represents the mass deficiency within the boundary layer.A new boundary for inviscid flow, which accounts for boundary-layer effects, can be established by adding a displacement surface to the body surface. This surface, known as the displacement surface, can lead to improvements in inviscid flow solutions when the deviation from the original surface is significant enough to warrant the inclusion of viscous effects in the inviscid flow equations[3].

An efficient and commonly used method, elaborated in reference [3], for studying aerodynamic flows involves the concept that the displacement surface can be effectively formed through the distribution of blowing or suction velocity on the body surface.The strength of the blowing or suction velocity v_b is determined from the boundary-layer solutions according to

$$v_b = \frac{d}{dx}\left(u_e \delta^*\right)$$

where *x* is the surface distance of the body, and the variation of v_b on the body surface implies that the boundary of the potential flow becomes the displacement (δ^*) surface and thereby takes account of the viscous effects in the potential-flow solution.

Taking a high aspect ratio wing as a case study, the aerodynamic coefficient is calculated using both the unsteady three-dimensional panel method and the coupled PM-BL approach. The results are then compared with CFD simulations in order to verify the accuracy of the viscosity correction. The geometric features of the wing are as follows: as shown in Fig.4, the half-span is 1542.1mm, the root chord is 263.24mm, the tip chord is 70.92mm, and the sweep angle is 3.4°. The airfoil adopts supercritical airfoil, as shown in Fig.5.At the same time, there is an initial torsion angle of 2° between the wing root and the wing tip, an angle of 2.242° between the front and rear edge points of the wing root profile and the x-axis, and an Angle of 0.229° between the front and rear edge points of the wing tip profile and the x-axis.

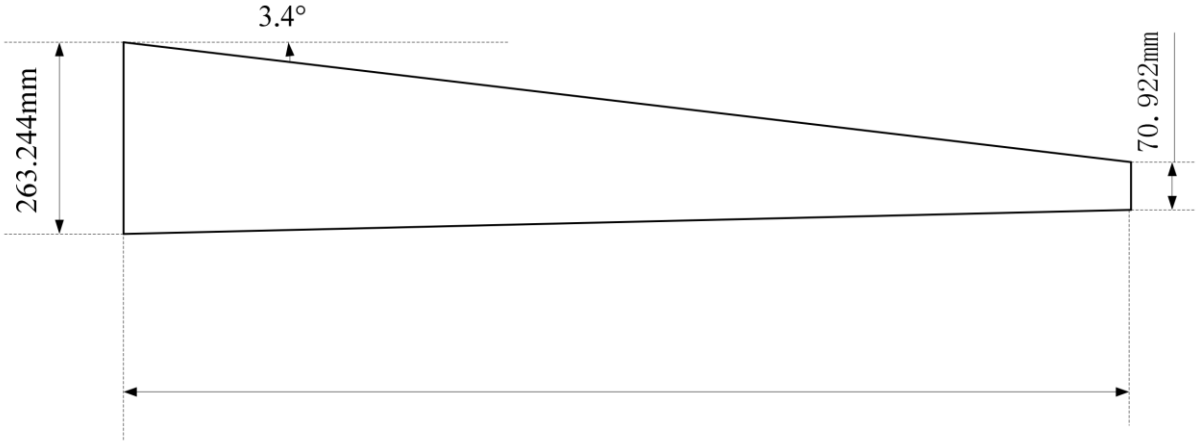

Figure 4 wing planform

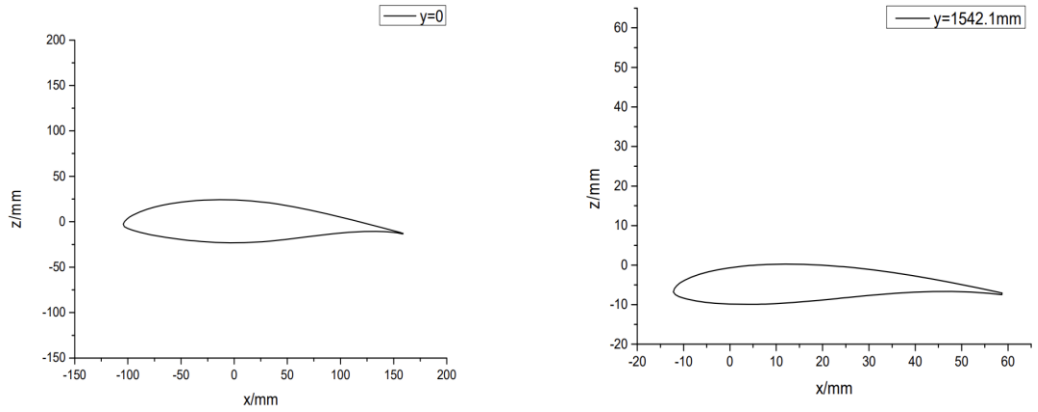

Figure 5 wing airfoil

The calculated working condition is inflow velocity 30m/s, and $Re = 3\times10^5$. The angle of attack of the wing root undergoes a rotational harmonic motion $\alpha = 3^\circ + 0.5^\circ sin(20\pi t)$.The 3D panel method model divides the upper and lower surfaces of the wings into meshes, the airfoil section is divided into 60 meshes and the spanwise section into 50 meshes, and a total of 3000 aerodynamic meshes are divided. The whole CFD flow field is meshed with 2,000,000 hexahedral meshes, SA turbulence model is adopted. The analysis results of the lift coefficient and drag coefficient of the wing are shown in Fig.6. It can be seen that the lift coefficient and drag coefficient obtained based on the coupled PM-BL approach are basically consistent with the analysis accuracy of CFD, but the calculation time is still roughly equivalent to that of the 3D panel method.

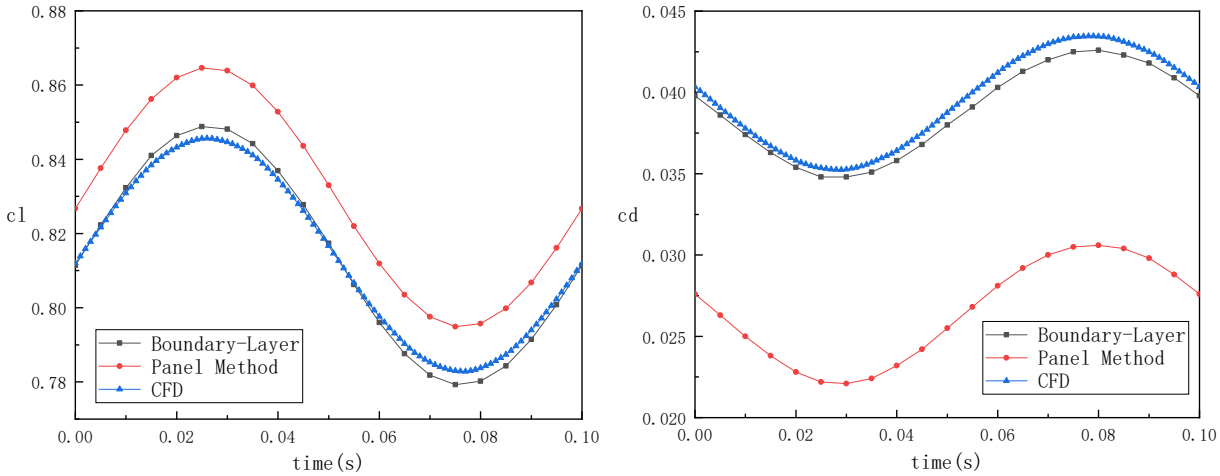

Figure 6 Analysis results of the coupled PM-BL approach

4 CONCLUSIONS

Represented by high-altitude long-endurance UAVs and large transport aircraft, large flexible aircraft with high-aspect-ratio wing layouts have become the design and development trend of advanced aircraft. Due to the wide application of lightweight composite materials, large flexible wings will deform greatly under flight loads and have significant nonlinear aeroelastic effects.

In this paper, a coupled PM-BL method is developed for unsteady aerodynamic analysis based on the aerodynamic modeling method of large flexible wings. The results show that the accuracy of the coupled PM-BL approach for a high aspect ratio wing is essentially equivalent to that of the CFD method, and the computation time on a standard desktop computer is measured in minutes.

REFERENCES

[1] Cebeci, T., Analysis of Turbulent Flows, Elsevier, London, 2004.

[2] Katz J, Plotkin A. Low-speed aerodynamics [M]. McGraw-Hill Inc, 1991.

[3] Cebeci, T., An Engineering Approach to the Calculation of Aerodynamic Flows, Horizons Pub., Long Beach, Calif., and Springer, Heidelberg, 1999.

COPYRIGHT STATEMENT